UKACC International Conference on Control 2012
Cardiff, UK, 3-5 September 2012

Stability control of a railway vehicle using absolute stiffness and inerters

Alejandra Z. Matamoros-Sanchez,
Roger M. Goodall
and Argyrios C. Zolotas
School of Electronic, Electrical and
Systems Engineering. Loughborough University
Loughborough, United Kingdom LE11 3TU
Email: {A.Z.Matamoros-Sanchez,
R.M.Goodall, A.C.Zolotas}@lboro.ac.uk

Jason Zheng Jiang
and Malcolm C. Smith
Department of Engineering
University of Cambridge
Cambridge, United Kingdom CB2 1PZ
Email:{z.jiang, mcs}@eng.cam.ac.uk

***Abstract*—Work presented in this paper studies the potential of employing inerters –a novel mechanical device used successfully in racing cars– in active suspension configurations with the aim to enhance railway vehicle system performance. The particular element of research in this paper concerns railway wheelset lateral stability control. Controlled torques are applied to the wheelsets using the concept of absolute stiffness. The effects of a reduced set of arbitrary passive structures using springs, dampers and inerters integrated to the active solution are discussed. A multi-objective optimisation problem is defined for tuning the parameters of the proposed configurations. Finally, time domain simulations are assessed for the railway vehicle while negotiating a curved track. A simplification of the design problem for stability is attained with the integration of inerters to the active solutions.**

***Index Terms*—Railway vehicles, wheelsets stability control, absolute stiffness, active suspensions, inerter.**

I. Introduction

A range of challenges is present in the design of modern railway vehicles, which are rather complex mechanical systems. Over the past thirty years, the use of sensors, electronic controllers, and actuators technology has enabled important changes in modern trains to deal with some of those difficulties hence enhancing vehicle system performance capabilities. In this context, the introduction of "active suspension" solutions, either in complementing or replacing conventional passive suspensions, did play a major role [1]. Conventional passive suspensions, via the vehicle geometry, both define important vehicle dynamics characteristics and are subject to operational constraints and limitations mainly due to the mechanical setup (e.g. combinations of springs, dampers, or pneumatic suspensions, and related mechanical linkages).

Admitting the role of passive suspensions as mechanical compensators of the vehicle's bodies dynamic interaction, a dominant factor in the overall performance results is in the type of structures that can be synthesised using simple elements like springs and dampers. Moreover, the nature of passive suspensions constrains the set of variables available for mechanical feedback. This highly determines the kind of resultant forces applied on the bodies and may cause some undesirable coupling between the system modes.

The use of active suspensions, i.e. usually the introduction of a controlled force-element (actuator), does offer enhanced suspension performance and some flexibility in the way the suspension structure evolves (actuator location and characteristics). However, this approach introduces the issue of energy consumption of the controlled element. Dynamic performance encompasses the problems associated to ride quality, dynamic stability and response to track features (e.g. curved sections of the rail track), for which active suspensions have been shown to facilitate higher speed and/or reduced track interaction [2]. Notwithstanding that active technologies cover a wide range of solutions for railway vehicles dynamic, passive compensation possibilities have grown with the introduction of the *inerter* [3]. The inerter is a novel concept and mechanical device with kinetic energy storage capabilities. This concept has been employed in automotive applications (being very successful in Formula 1 ™ cars [4]), in motorcycles [5] and in building suspension control [6]. Also, there have been recent discussions on the use of inerters in pure passive railway suspension performance enhancement (see for example [7]).

This paper studies an approach that is different to the ones arising from current literature on inerters for railway vehicles. In particular, it investigates the performance merits of introducing the inerter together with the concept of active stability control of wheelsets via the absolute stiffness approach [8].

II. Railway vehicle dynamics

Motions in a railway vehicle normally accept a certain degree of separation for suspension design and performance assessment purposes (for a typical railway vehicle schematic refer to Fig. 1). The study in this paper concerns wheelset stability control, and hence the modelling refers to only the lateral and yaw vehicle dynamic characteristics. Lateral and yaw motions are usually controlled by primary suspensions,

A. Z. Matamoros-Sanchez gratefully acknowledges the support of Universidad de Los Andes, Venezuela and Loughborough University, UK.
The work of J. Z. Jiang and M. C. Smith was supported by the Engineering and Physical Sciences Research Council grant number EP/G066477/1.

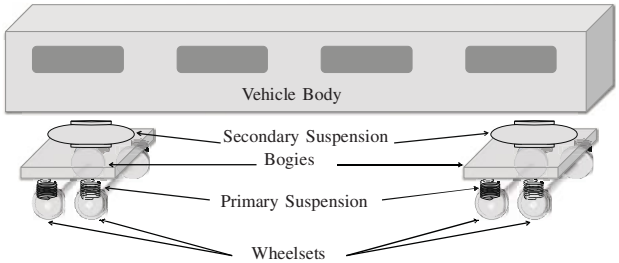

Fig. 1. Bodies and suspension stages of a railway vehicle.

with the main concern being the vehicle running behaviour at the wheel-rail interface, for which a design conflict between the vehicle stability and curving performance exists. Bruni et al. [2] presented a survey on the concepts and trends on active suspensions, where a detailed description of the control strategies for active primary suspensions is provided. They explain the essential kinematic instability of the solid axle wheelsets of the railway vehicle. Active solutions based on either lateral or yaw actuation controlled by feedback of yaw angles or lateral velocities re-locate the unstable poles of the wheelsets to the stable semi-plane. Yaw damping, both relative and absolute yaw stiffness, and lateral damping are some of the previously studied and widely known stabilising solutions in this field. The current study considers the application of relative yaw stiffness with the use of novel mechanical devices, in the search for complementing the active control strategy based on absolute yaw stiffness. The design of both structures is integrated so that they provide a synergetic solution.

Besides stability, the forces emerging from the wheel-rail interface when wheelsets negotiate curved tracks impose additional requirements to the design, albeit the control solutions for this aim are normally separated from the stability solutions. Steering control is dedicated to the 'perfect curving' [2], targeting: a) equal lateral creep forces on all the wheelsets to minimise track shifting forces, and b) zero steady-state longitudinal creep forces on all wheelsets. Some lateral creep is required in order to provide the necessary force to counterbalance the centrifugal force on curves [9], while longitudinal creep forces are associated to wear and noise and thus the requirement design is to significantly reduce them. Some steering solutions are also summarised in [2].

This paper assesses the curving behaviour as an outcome of the synergy between novel passive and active solutions designed for stability. Although some conditions in the overall design are established in regard to the steering problem, it is not defined as control objective for the active solution.

III. Mathematical model of the system

The mathematical model approximating the lateral and inherent dynamics of a railway vehicle can be described by linear differential equations. The modelling is based upon the plan-view schematic representation presented in Fig.1. The use of linearised models is a normal practice in the design of active controllers, justified by the fact that active solutions reasonably overcome the effects of nonlinearities associated with the rail-wheel contact effects and other sources of nonlinear behaviour [10], in particular avoiding significant contact between the wheel flange and the rail. The mathematical description employed here for the assessment of a railway vehicle stability control corresponds to half of the vehicle comprising a two-axle bogie and half vehicle body. Primary and secondary suspensions in the vehicle provide the vertical linkages between the solid-axle wheelsets and the bogie frame, and the bogie frame and the vehicle body, respectively (Fig. 1). In the model, the lateral and longitudinal stiffness of the primary suspension are considered. Although the lateral primary damping is also modelled, the longitudinal is neglected. Likewise, the lateral stiffness and damping of the secondary suspension are included. The wheelsets consist of two wheels with conical profile rigidly joined together through a common axle, for which a nominal —ideally invariable— conicity coefficient, λ, and radius, r_0, are assumed. Rail/wheels interaction is taken into account through the longitudinal and lateral creep forces with ideally constant creep coefficients, f_{11}, and f_{22}. The creep forces arise at the contact points as consequence of the difference in strain rates of the wheels and the track (Fig. 2) –see Garg and Dukkipati [11] for an extended explanation. For every wheelset, those are given by:

$$F_x = 2f_{11}l_{wy}\left(\frac{1}{R} - \frac{1}{V}\dot{\theta}_w\right) - \frac{2f_{11}\lambda}{r_0}\left(y_w + y_t\right) \quad (1)$$

$$F_y = -2f_{22}\left(\frac{\dot{y}_w}{V} - \theta_w\right) \quad (2)$$

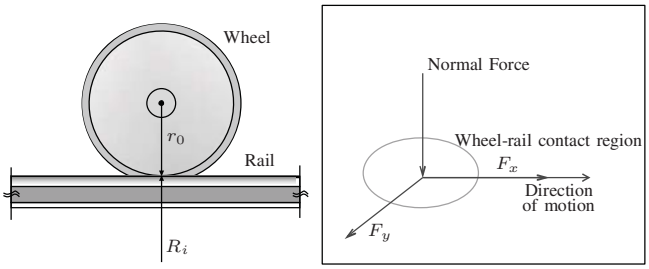

Fig. 2. Left: principal wheel and rail radii of curvatures. Right: Longitudinal and lateral creep forces.

Table I lists the parameters and the corresponding numerical values, while the schematic diagram of a wheelset is shown in Fig. 3. The differential equations (3)-(8) represent the dynamics of the seven degrees-of-freedom of the vehicle, namely: the lateral displacement and yaw angle of the wheelsets, respectively y_{wi} and θ_{wi} for i=1, 2 (1: front, 2: rear), and the bogie, respectively y_b and θ_b, and also the vehicle body lateral motion y_v. This model with the default parameters values is equivalent to that used by Jiang et al. [12], except for the disregarded longitudinal primary damping and that the steering

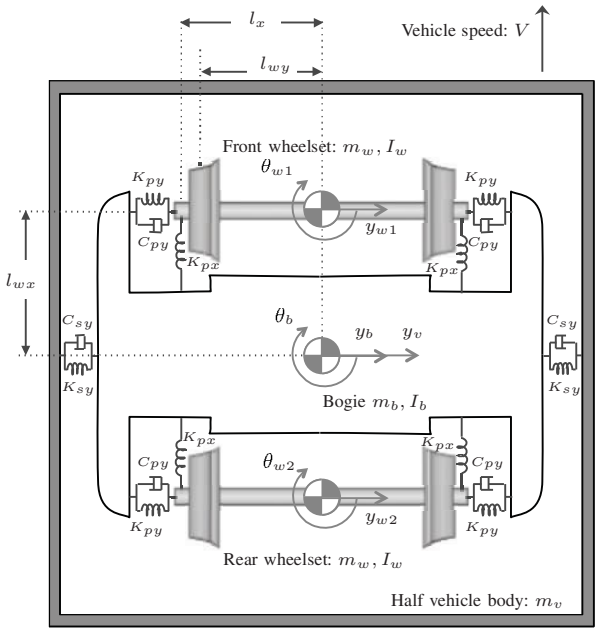

Fig. 3. Plan-view of the railway vehicle.

TABLE I
NOMINAL PARAMETERS VALUES OF THE HALF-VEHICLE MODEL

Symbol	Description
V	Vehicle speed (55ms^{-1})
m_w	Wheelset mass (1376 kg)
I_w	Wheelset yaw inertia (766 kgm^2)
m_g	Bogie frame mass (3477 kg)
I_g	Bogie frame yaw inertia (3200 kgm^2)
m_v	Half vehicle body mass (17230 kg)
r_0	Wheel radius (0.445 m)
λ	Wheel conicity (0.3)
f_{11}	Longitudinal creepage coefficient (10^7 N)
f_{22}	Lateral creepage coefficient (10^7 N)
l_{wx}	Semi-longitudinal spacing of wheelsets (1.225 m)
l_{wy}	Half gauge of wheelset (0.75 m)
l_x	Semi-lateral spacing of steering linkages and primary longitudinal suspension (1.2 m)
K_{px}	Primary longitudinal stiffness per axle box (10^6 Nm^{-1})
K_{py}	Primary lateral stiffness per axle box (4.71×10^6 Nm^{-1})
C_{py}	Primary lateral damping per axle box (1.2×10^4 Nsm^{-1})
K_{sy}	Secondary lateral stiffness per axle box (2.45×10^5 Nm^{-1})
C_{sy}	Secondary lateral damping per axle box (2×10^4 Nsm^{-1})
R_i	Radius of the curved track (1000 m)
$\theta_{c,i}$	Cant angle of the curved track ($6 \times \pi/180$ rad)
g	Gravity (9.81ms^{-2})

linkage is not included.

$$\begin{aligned} m_w\ddot{y}_{w,i} =& 2K_{py}\left(y_b + (-1)^{i-1} l_{wx}\theta_b - y_{w,i}\right) + F_{y,i} \\ &+ 2C_{py}\left(\dot{y}_b + (-1)^{i-1} l_{wx}\dot{\theta}_b - \dot{y}_{w,i}\right) \quad (3) \\ I_w\ddot{\theta}_{w,i} =& 2K_{px}l_x^2\left(\theta_b - \theta_{w,i}\right) + l_{wy}F_{x,i} \\ &+ 2\,l_x^2 F_{pn,i} + \tau_{u,i} \quad (4) \\ m_b\ddot{y}_b =& 2K_{py}\left(y_{w1} + y_{w2} - 2y_b\right) + 2K_{sy}\left(y_v - y_b\right) \\ &+ 2C_{py}\left(\dot{y}_{w1} + \dot{y}_{w2} - 2\dot{y}_b\right) + 2C_{sy}\left(\dot{y}_v - \dot{y}_b\right) \\ &+ \frac{m_b V^2}{2}\left(\frac{1}{R_1} + \frac{1}{R_2}\right) - m_b g\left(\frac{\theta_{c1} + \theta_{c2}}{2}\right) \quad (5) \\ I_b\ddot{\theta}_b =& 2K_{py}l_{wx}\left(y_{w1} - y_{w2} - 2l_{wx}\theta_b\right) \\ &+ 2K_{px}l_x^2\left(\theta_{w1} + \theta_{w2} - 2\theta_b\right) \quad (6) \\ &+ 2C_{py}l_{wx}\left(\dot{y}_{w1} - \dot{y}_{w2} - 2l_{wx}\dot{\theta}_b\right) \\ &- 2\,l_x^2\left(F_{pn1} + F_{pn2}\right) - \tau_{u1} - \tau_{u2} \quad (7) \\ m_v\ddot{y}_v =& 2K_{sy}\left(y_b - y_v\right) + 2C_{sy}\left(\dot{y}_v - \dot{y}_v\right) \\ &+ \frac{m_v V^2}{2}\left(\frac{1}{R_1} + \frac{1}{R_2}\right) - \frac{m_v g}{2}\left(\theta_{c1} + \theta_{c2}\right) \quad (8) \end{aligned}$$

It is noticeable from the model above that the suspensions in the longitudinal direction affect the wheelsets and bogie yaw mode only. This is explained by the symmetric allocation of those suspensions in the plane with respect to the centre of gravity of the bogie and every wheelset. That partly justifies the structure of the active control configuration exposed later.

For simulations and optimisation purposes, the state-space representation of this open-loop model was derived as

$$\begin{aligned} \dot{x} &= A\,x + B\,u + B_\eta\,\eta \\ y_o &= C_o x \\ y_m &= C_m x \end{aligned} \quad (9)$$

with

$$\begin{aligned} x =& [\dot{y}_{w1},\, y_{w1},\, \dot{\theta}_{w1},\, \theta_{w1},\, \dot{y}_{w2},\, y_{w2},\, \dot{\theta}_{w2},\, \theta_{w2},\, \ldots \\ & \dot{y}_b, y_b, \dot{\theta}_b, \theta_b, \dot{y}_v, y_v]^T \\ u =& [\tau_{u1},\, \tau_{u2},\, F_{pn1},\, F_{pn2})^T \\ \eta =& [1/R_1,\, \theta_{c1},\, y_{t1},\, 1/R_2,\, \theta_{c2},\, y_{t2}]^T \\ y_o =& [F_{x1},\, F_{x2},\, F_{y1},\, F_{y2}]^T \\ y_m =& [\theta_{w1},\, \theta_{w2},\, \dot{\theta}_b - \dot{\theta}_{w1},\, \dot{\theta}_b - \dot{\theta}_{w2}]^T, \end{aligned}$$

where u is the vector of the active and passive control inputs applied to the system, η are the exogenous inputs from the railway track, y_o are the outputs related to the performance of the excited system, and y_m are the variables/measurements to be fed back through the passive and active control configurations described in this paper.

IV. ABSOLUTE STIFFNESS FOR STABILITY CONTROL

Highly stiff passive connections in the longitudinal direction between every axle and the bogie frame of a railway vehicle are known to provide the required levels of wheelset stability at high speeds on straight tracks [1]. However, since the bogie is relatively light, the two wheelsets and bogie become strongly

coupled. The consequence is that an even higher longitudinal stiffness is necessary to achieve satisfactory stability levels, but because this stiffness also affects curving performance there is an increase in wheel and rail wear.

Mei and Goodall in [8] presented a more effective implementation for stiffness-based stabilisation in contrast with the conventional passive stiffness, the absolute stiffness –*skyhook stiffness* approach. This is an active configuration in which a longitudinal/yaw force/torque proportional to the high-pass filtered absolute wheelset yaw angle is applied between every wheelset and the bogie frame. The strategy decouples the wheelsets dynamic, preventing their stability being affected by the bogie dynamic and hence overcoming the complexity of the wheelsets stabilisation due to the wheelsets and bogie interaction. As pointed out by Mei and Goodall [8] the use of pure absolute yaw stiffness would cause problems for curving, so the high-pass filtering is necessary. In this manner absolute stiffness is an appealing solution to the stability problem.

The implementation of the strategy in this approach consists of the measurement of the wheelsets' yaw angles, which are filtered using individual second order high-pass filters of the same cut-off frequency, and are fed-back through a proportional controller to the respective actuators mounted between the wheelsets axles and the bogie frame applying the control torques, as represented in Fig. 4 and Eq. (10):

$$\hat{\tau}_{u,i}{=}{-}K_u \left(\frac{{}^{s^2}\!/_{(2\pi f_c)^2}}{{}^{s^2}\!/_{(2\pi f_c)^2} + {}^{1.414\,s}\!/_{2\pi f_c} + 1} \right) \hat{\theta}_{w,i} \qquad (10)$$

The controllable realisation of (10) is obtained in A_τ, B_τ, C_τ, D_τ for a definition of the individual sub-systems (i.e. front—$i = 1$ and rear—$i = 2$ controllers) in the state-space as

$$\begin{aligned} \dot{x}_{\tau,i}{=}A_\tau\, x_{\tau,i} + B_\tau\, \theta_{w,i} \\ \tau_{u,i}{=}C_\tau\, x_{\tau,i} + D_\tau\, \theta_{w,i} \end{aligned} \qquad (11)$$

Variants of the implementation would be the estimation of the wheelsets yaw angle if the physical measurements are difficult to obtain, and/or to use linear actuators in the longitudinal direction instead of rotational ones. In this paper, the availability of the measurements and ideal actuators were supposed. Note, however, that Mei and Goodall [8] explain how a robust yaw gyro might effectively be used to derive the high-pass filtered yaw angle. Also in [8] Mei and Goodall point out the analogy between absolute stiffness and a "skyhook spring", i.e. a spring virtually connected between the wheelset and the "sky". As the authors noted in their paper [8], the analogy is not exact since in any practical implementation through a linear or rotational actuator there must be an equal and opposite reaction/force between the wheelset and bogie. The true reaction forces/torques are shown in Fig. 4 and implemented in the dynamic equations (3)-(8).

V. Absolute stiffness control and inerters

In this research, there is an interest on studying the potential of creating a synergy between passive and active solutions for railway vehicles dynamics, especially with the use of inerters, a recent concept in mechanical devices. Thereby, in combination with the active stability control strategy exposed above, different passive suspensions allocated in the longitudinal direction are proposed as represented in Fig. 5. The objective is to enhance the active solution through arbitrary passive networks, for which a cooperation between the two schemes is desirable to increase the possibilities of guaranteeing stability using absolute stiffness.

In the previous section, a description of two solutions for the bogie stability problem was provided, based on the use of passive and active stiffness. After having exposed that one of the major difficulties of applying either yaw or longitudinal stiffness alone between the wheelsets and the bogie is the response during curving, a frequency-based focus is provided

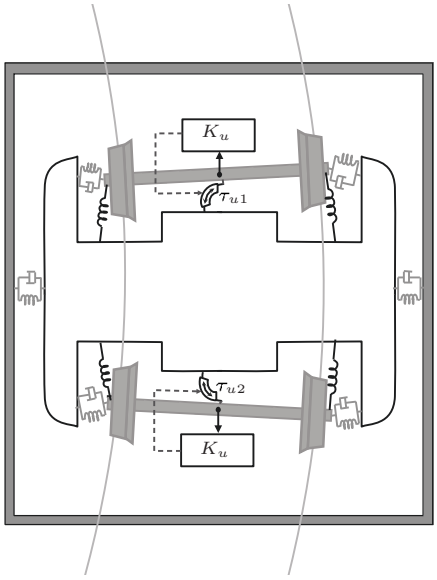

Fig. 4. Absolute stiffness stability control.

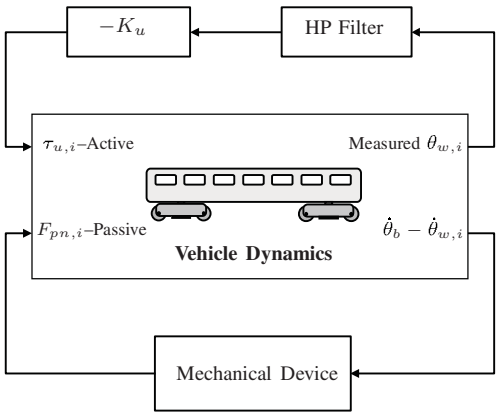

Fig. 5. Block diagram representation of absolute stiffness and novel mechanical devices integration.

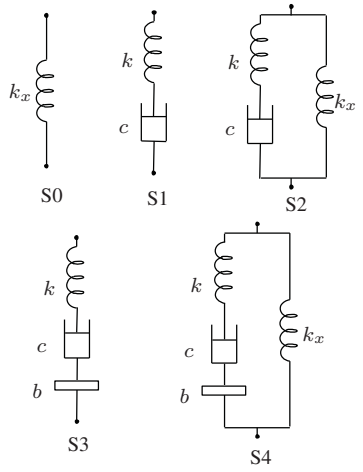

Fig. 6. Candidate suspension layouts.

in this section to introduce the role of more extensive passive suspensions.

In general, rail geometry characteristics in the lateral direction can be separated into high frequency for stochastic irregularities (predominant in straight tracks), and low frequency for curves. In fact, for the application of absolute stiffness it was already mentioned that high-pass filtering would alleviate the issues arising on curving. From the control perspective, the frequency response of mechanical suspensions is clearly a distinctive fact. For example, a linear spring has a flat frequency response to relative displacements between its terminals; this has a counterpart for the vehicle's behaviour which was identified earlier in this paper. In that sense, a non arbitrary range of passive networks can be designed using springs and dampers only to 'relax' the longitudinal stiffness at certain frequencies. However, the possibilities are reduced in the design of convenient configurations. A wider freedom on the design of passive suspensions using simple mechanical elements properties was given by the introduction of the inerter concept.

An inerter is a two-terminal mechanical device analogous to an ungrounded capacitor in an electric circuit, according to the force-current analogy, as described by Smith in [3]. It develops a linear force at its terminals which is proportional to the relative acceleration across them. It was termed by Chen et al. [4] to be 'the missing mechanical element' required to complete the referred analogy with electric networks using resistors, inductors and capacitors only, for which arbitrary passive impedances can be synthesised. In this manner, the inerter extends the possibilities in the synthesis of mechanical impedances and equivalently allows the formulation of arbitrary frequency characteristics with the unique constraint being on positivity requirements [3].

In this study, simple layouts using springs, dampers and inerters are examined. The candidate layouts basically consider the introduction of a novel mechanical device in the longitudinal plane with different stiffness according to the excitation frequency, augmenting the longitudinal stiffness already provided by the primary suspensions. Those are represented in Fig. 6, for which the parameter b is the inertance property of the inerter, with units given in kilograms. c, k, and k_x stand for normal damping and stiffness design parameters. The passive forces applied on the wheelsets and the bogie are characterised by the candidate layouts complex mechanical admittance Y_{pn}(see [3]) as follows

$$\hat{F}_{pn,i}=\mathrm{Y}_{pn}s\,(\theta_b-\theta_{w,i}) \tag{12}$$

TABLE II
COMPLEX ADMITTANCE OF THE CANDIDATE LAYOUTS IN FIG. 6

Layout	Complex Admittance, $\mathrm{Y}_{pn}(s)$
S0	$\frac{k_x}{s}$
S1	$\frac{c}{c/k\,s+1}$
S2	$\frac{k_x}{s}+\frac{c}{c/k\,s+1}$
S3	$\frac{b\,s}{b/k\,s^2+b/c\,s+1}$
S4	$\frac{k_x}{s}+\frac{b\,s}{b/k\,s^2+b/c\,s+1}$

The complex admittance of every layout is given in Table II. For every passive layout, the controllable canonical form was obtained in A_{pn}, B_{pn}, C_{pn}, D_{pn}, which is common to the two subsystems generating the longitudinal forces F_{pn1} and F_{pn2} in response to $\dot{\theta}_b-\dot{\theta}_{w1}$ and $\dot{\theta}_b-\dot{\theta}_{w2}$, respectively, and with states vectors x_{pn1} and x_{pn2} .

Although this reduced selection of passive structures does not allow to generalise on the effect of the inerter in passive longitudinal suspensions combined with active yaw control, it identifies the potential of the inerter in this proposed synergy.

VI. Optimisation of parameters and performance assessment

Once the structure of the controllers has been established, both active and passive, a multi-objective optimisation problem was formulated on the closed-loop system represented in the state-space as

$$\begin{aligned}\dot{x}_{cl}&=\mathcal{A}x_{cl}+\mathcal{B}_\eta\eta\\ y_{cl}&=\mathcal{C}x_{cl}\end{aligned} \tag{13}$$

for the augmented state vector

$$x_{cl}=\left[x^T\middle|x_{\tau1}^T\middle|x_{\tau2}^T\middle|x_{pn1}^T\middle|x_{pn2}^T\right]^T, \tag{14}$$

and the output vector $y_{cl}=y_o$ re-written accordingly. The closed-loop system's matrices are defined as

$$\begin{aligned}\mathcal{A} &= \left[\begin{array}{c|c}A+B\,\Lambda_D^u C_m & B\,\Lambda_C^u\\ \hline \mathcal{A}_{21} & \Lambda_A^u\end{array}\right],\\ \mathcal{B} &= \left[\begin{array}{c|c|c|c} B_\eta^T & 0 & 0 & 0\end{array}\right]^T, \text{and}\\ \mathcal{C} &= \left[\begin{array}{c|c|c|c} C_o & 0 & 0 & 0\end{array}\right],\end{aligned}$$

with

$$\Lambda_A^u = \text{diag}\,(A_\tau,\, A_\tau,\, A_{pn},\, A_{pn})$$
$$\Lambda_C^u = \text{diag}\,(C_\tau,\, C_\tau,\, C_{pn},\, C_{pn})$$
$$\Lambda_D^u = \text{diag}\,(D_\tau,\, D_\tau,\, D_{pn},\, D_{pn})\,,$$

and

$$\mathcal{A}_{21} = \left[\; C_{m(1,*)}^T B_\tau^T \,\middle|\, C_{m(2,*)}^T B_\tau^T \,\middle|\, C_{m(3,*)}^T B_{pn}^T \,\middle|\, C_{m(4,*)}^T B_{pn}^T \;\right]^T .$$

The "zero" entries in the matrix definitions are zero vectors/matrices of appropriate dimension, and $C_{m(i,*)}^T$ corresponds to the i-th row of the matrix C_m in (9).

In the stability problem devised for optimisation, two additional design objectives compromise the optimum stability: the minimisation of the active control gain and the minimisation of the fixed parallel stiffness k_x for the layouts S0, S2 and S4. With this, one aims to determine whether or not the use of passive suspensions with inerters allows the reduction of the control gain and to improve the vehicle's performance while curving. The objective for an optimum stability was defined as the maximisation of the least damping ratio among the kinematic modes of the vehicle at a particular travelling speed of V=55ms^{-1} (approx. 200km/h).

The Matlab® genetic algorithms (GA) toolbox was utilised to solve the trade-off emerging from this multiple goals formulation. The tuning parameters in the problem were: the control gain, K_u, the cut-off frequency of the high-pass filter, f_c, and the stiffness, damping and inertance parameters according to each individual candidate layout. Reasonable values for the physical constraints on the parameters were supplied to the algorithm. Because the optimum stability definition for the nominal speed does not necessarily account for lower speeds stability, a penalty was included in the stability cost function based on dismissing the parameter set for which the vehicle was unstable at the particular speed of 5ms^{-1}. Even though it does not avoid instability for all the speeds below the nominal, it does provide certain level of control on the stability along the evaluated range of speeds without significantly affecting the optimal tuning for the nominal speed. Indeed, with this procedure, levels of instability –possibly unrealistic– occur only for very low speeds which are transitional for a high-speed train running at normal conditions.

A. Optimal stability

For the stability control design, the vehicle was considered to travel on a straight track, i.e. the curved track radius $R_i \to \infty$, and consequently also zero cant angle, $\theta_{c,i}$, for i=1, 2 (radius and cant angle measured at the front and rear wheelsets positions). The 3D plot in Fig. 9 shows the best population attained with genetic algorithms for those candidate layouts including k_x. It evidences the conflict between the three objectives defined in the study. The 3D plot reveals how the inerter simplifies the optimisation problem resulting with longitudinal stiffness values, k_x, between $0 - 2 \times 10^6 \text{Nm}^{-1}$, and control gain values, K_u, between $(10 - 20) \times 10^6$. Conversely, for the suspensions S0 and S1 the algorithm encountered different settings providing the same stability level with greater variability in the components parameters values. Decisions on the optimisation results are compiled in Table III, indicating also the best value for the least damping ratio, ζ_c, at the design speed. The choice of the best set of parameters was arbitrarily done on the highest stability index value, ζ_c. For those suspensions without the inerter the optimum set was chosen to be the one with the highest level of stability and lowest stiffness. For S3 and S4 the best stability resulted for a single set of parameters in every case, thus those were the chosen for comparisons. Because the values of k_x and K_u are reasonable, this method of choosing the best settings focused mostly on the degree of stability. Achievements are contrasted with the default passive configuration in Fig. 3 (equivalent to S0 with $k_x = 0$) with active stability control.

TABLE III
PARAMETERS VALUES FROM THE OPTIMISATION

Configuration	ζ_c **[%]**	**Active Optimal parameters**	**Passive Optimal parameters**
Default Active	20.6	$K_u = 1.37 \times 10^7$ $f_c = 0.001$ Hz	N/A
Active and S0	20.6	$K_u = 2.28 \times 10^7$ $f_c = 0.70$ Hz	$k_x = 6.39 \times 10^6$ Nm^{-1}
Active and S1	20.7	$K_u = 1.57 \times 10^7$ $f_c = 0.03$ Hz	$k_x = 0$, $c = 6.42 \times 10^5$ Nsm^{-1}, $k = 2.20 \times 10^6$ Nm^{-1}
Active and S2	20.8	$K_u = 4.94 \times 10^7$ $f_c = 0.76$ Hz	$k_x = 7.16 \times 10^6$ Nm^{-1}, $c = 58.83 \times 10^5$ Nsm^{-1}, $k = 2.55 \times 10^6$ Nm^{-1}
Active and S3	21.2	$K_u = 1.89 \times 10^7$ $f_c = 0.34$ Hz	$k_x = 0$, $c = 6.13 \times 10^5$ Nsm^{-1}, $b = 9.98 \times 10^4$ kg, $k = 2.55 \times 10^6$ Nm^{-1}
Active and S4	23.2	$K_u = 1.91 \times 10^7$ $f_c = 0.28$ Hz	$k_x = 0.78 \times 10^6$ Nm^{-1}, $c = 5.83 \times 10^5$ Nsm^{-1}, $b = 6.84 \times 10^5$ kg, $k = 2.77 \times 10^6$ Nm^{-1}

A classification of the candidate structures in Fig. 6 was done in two groups, A and B, for the presentation of the results: group A comprising novel devices without a fixed stiffness in parallel, i.e. S1 and S3, and group B consisting of novel devices with additional stiffness in parallel, i.e. S0, S2, and S4. The plots for ζ_c versus travelling speed with the optimum tuning obtained for the nominal speed V are depicted in Fig. 7 and Fig. 8, providing also a comparison with the stability curve for the passive conventional system. The passive conventional setting is for a steering linkage stiffness of $k_x = 3.666 \times 10^7\,\text{Nm}^{-1}$, guaranteeing the bogie stability, and τ_{u1} and τ_{u2} equal to zero.

From Fig. 7–8, improved stability achieved with all the configurations including active control can be observed. Particularly, those with inerters were found to provide, at some

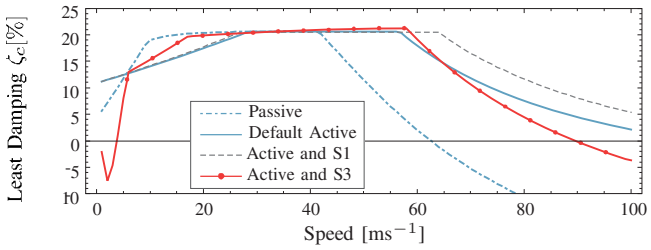

Fig. 7. Least damping ratio for the kinematic modes vs. speed (group A).

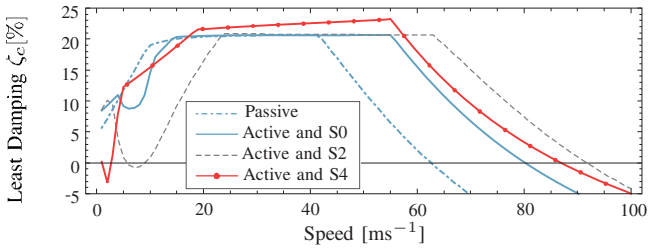

Fig. 8. Least damping ratio for the kinematic modes vs. speed (group B).

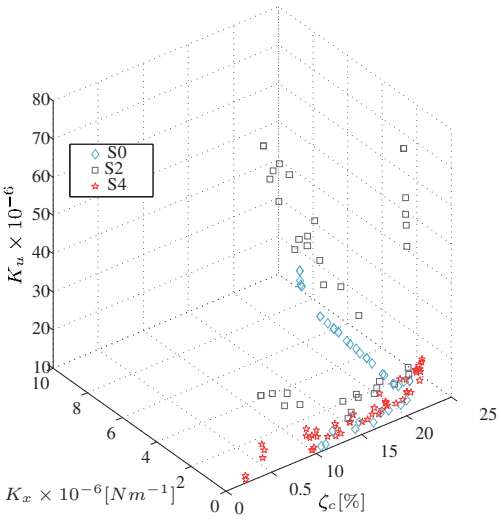

Fig. 9. Conflict 3D plot obtained from multi-objective optimisation for the active control combined with layouts in group B.

extent, a better improvement on the vehicle's stability at the nominal speed over the other configurations: about 3% with S3, and 12.6% with S4 compared with achievements with S0. Also for low speeds better stability is attained in contrast with the configurations using the "relaxed suspensions" S1 and S3, albeit the irrelevant instability obtained for speeds below 5ms^{-1}. For speeds above the design speed, the other configurations result with better stability. In this regard, other exercises were done on optimising for higher speeds and the tendency is to obtain a slightly better stability with S3 and S4 for the design speed in contrast to the results for the structures without the inerter.

B. Curving

With the optimum sets of parameters in Table III, curving behaviour in the time domain was also assessed. For this end, a track radius of 1000m and a cant angle of 6° were assumed, with a transition time of 3 seconds for a nominal travelling speed of V=55ms^{-1} as in Jiang et al.'s paper [12].

The system excited by these transitional inputs develops longitudinal and lateral forces as displayed in Fig. 10 and Fig. 11, with applied control torques as shown in Fig. 12 and Fig. 13. In Figs. 10-13, bold curves correspond to the front wheelset responses, while normal curves are for the rear wheelset. If one refers back to the complex admittance of the layouts in Fig. 6 (i.e. Table II) and the parameter values from the optimisation (Table III), one can find that the strength of the layouts S3 and S4 is the better attenuation of the low frequency content of the relative displacements between wheelsets and bogie in the development of the resultant passive forces. S3 and S4, i.e. the structures with an inerter, provide an attenuation of +40dB/dec in contrast with the +20dB/dec provided by S1 and S2, and the all-pass characteristic of S0. It causes the longitudinal suspensions to behave even softer while curving,

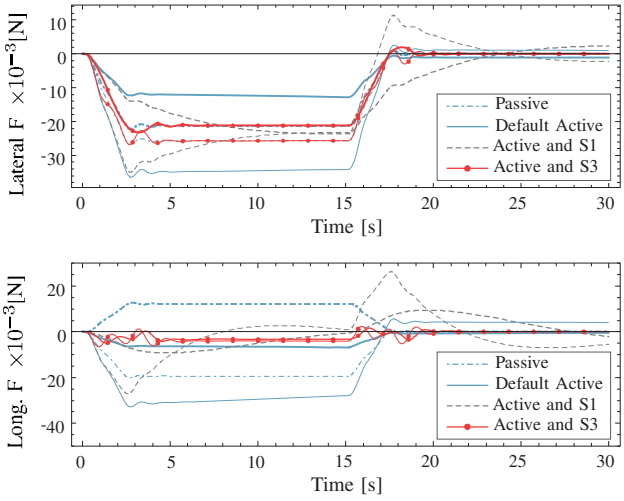

Fig. 10. Creep forces: Top- Lateral, Bottom- Longitudinal (group A).

and with a flat stiffness for high frequency components, e.g. track irregularities. The filter effect of every suspension system is encountered at the following cut-off frequencies: 3.4 rads^{-1} for S1, 0.4 rads^{-1} for S2, 5.1 rads^{-1} for S3, and 2 rads^{-1} for S4. It reveals lowered cut-off frequencies for the structures with a fixed stiffness placed in parallel to the softer structures (or equivalently, frequency-dependent stiffness).

Results from the optimisation disclose that the active control technique based on absolute position of the wheelsets feedback can be further improved by feeding back the position of the wheelsets relative to the bogie position with adequate compensation. Analysing the simulations for the creep forces

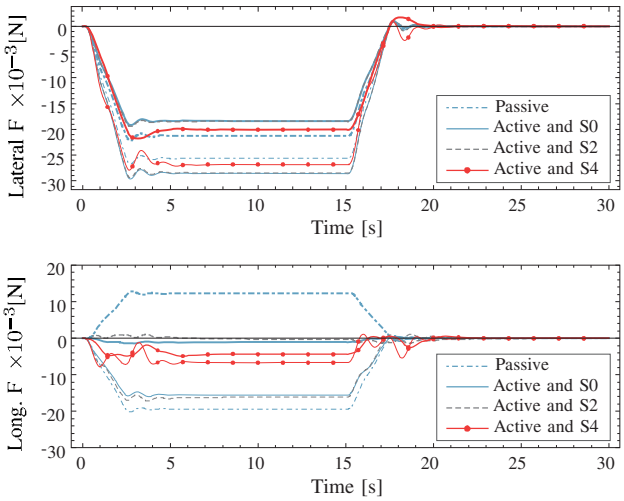

Fig. 11. Creep forces: Top- Lateral, Bottom- Longitudinal (group B).

and the active torques, the following benefits were obtained:

- a difference between the front and rear lateral creep forces for both S3 and S4 conveniently close to that obtained with the pure passive stabilisation configuration (for which ζ_c is approximately 7% only);
- a significant and favourable reduction of the front and rear longitudinal creep forces for both S3 and S4, when compared with those configurations without inerter, and
- lower active torque for S3, while higher for S4 –although perhaps better damped.

At higher nominal speeds, e.g. 83 ms^{-1} (300km/h), suspensions as S1 and S3 will not guarantee a high degree of stability; results are not included here for brevity. In those cases, a fixed stiffness is needed for all the frequencies and therefore S2 and S4 are more appropriate. In fact, Fig. 10 and Fig. 12 show that even at 55 ms^{-1}, S1 is not adequate.

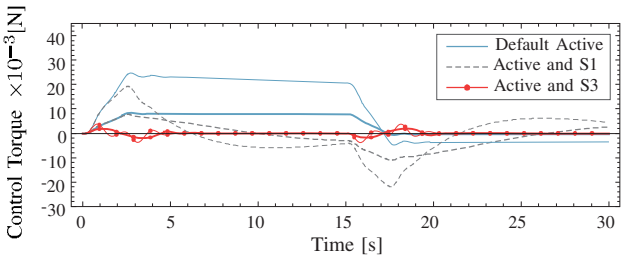

Fig. 12. Time-response for the applied control torque (group A).

VII. Conclusion

Including inerters into the longitudinal suspensions simplifies the issues arising in stability control of a railway vehicle using absolute stiffness. A best compromise was achieved for the three objectives formulated: maximum stability for the nominal travelling speed, and reduction of the longitudinal stiffness and the control gain via GA optimisation. Time

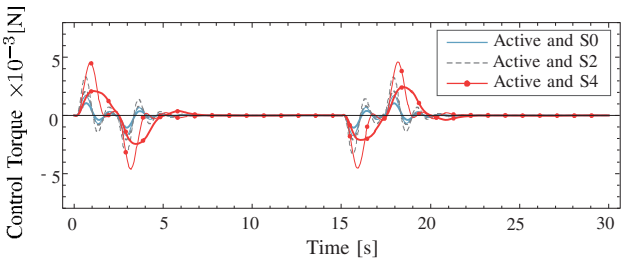

Fig. 13. Time-response for the applied control torque (group B).

domain simulation results illustrated the usefulness of adding the inerter to the active control solution, i.e. some improvement in the wheelsets stability was attained while also longitudinal and lateral creep forces are reduced. This study presented possibilities of enhancing railway suspension behaviour via active control integrated with a novel mechanical element, the inerter.

References

[1] S. Iwnicki, *Handbook of railway vehicle dynamics*. United States of America: CRC Press, 2006.

[2] S. Bruni, R. Goodall, T. X. Mei, and H. Tsunashima, "Control and monitoring for railway vehicle dynamics," *Vehicle System Dynamics*, vol. 45, no. 7-8, p. 743, 2007.

[3] M. C. Smith, "Synthesis of mechanical networks: The inerter," *IEEE Transactions on Automatic Control*, vol. 47, no. 10, p. 1648, 2002.

[4] M. Z. Q. Chen, C. Papageorgiou, F. Scheibe, F. cheng Wang, and M. C. Smith, "The missing mechanical circuit element," *Circuits and Systems Magazine, IEEE*, vol. 9, no. 1, pp. 10–26, 2009.

[5] S. Evangelou, D. J. N. Limebeer, R. S. Sharp, and M. C. Smith, "Mechanical steering compensators for high-performance motorcycles," *Journal of Applied Mechanics- Transactions of the ASME*, vol. 74, no. 2, p. 332, 2007.

[6] F. C. Wang, C.-W. Chen, M.-K. Liao, and M.-F. Hong, "Performance analyses of building suspension control with inerters," in *Decision and Control, 2007 46th IEEE Conference on*, 2007, p. 3786.

[7] F. C. Wang and M.-K. Liao, "The lateral stability of train suspension systems employing inerters," *Vehicle System Dynamics.*, vol. 48, no. 5, p. 619, 2009.

[8] T. X. Mei and R. M. Goodall, "Stability control of railway bogies using absolute stiffness: sky-hook spring approach," *Vehicle System Dynamics*, vol. 44, no. sup1, p. 83, 2006.

[9] S. Shen, T. X. Mei, R. M. Goodall, and J. T. Pearson, "A novel control strategy for active steering of railway bogies," in *UKACC Control 2004*, 2004.

[10] T. X. Mei and R. M. Goodall, "Recent development in active steering of railway vehicles," *Vehicle System Dynamics*, vol. 39, no. 6, p. 415, 2003.

[11] V. K. Garg and R. V. Dukkipati, *Dynamics of Railway Vehicle Systems*. United Kingdom: Accademic Press, 1984.

[12] J. Z. Jiang, A. Z. Matamoros-Sanchez, R. M. Goodall, and M. C. Smith, "Passive suspensions incorporating inerters for railway vehicles," *Vehicle System Dynamics*, 2012, in press.